Paper ID: FM-92

Boundary layer analysis along a stretching wedge surface in cylindrical coordinate

M. Ali[1]*, M. A. Alim[2] and R. Nasrin[2]

[1]Chittagong University of Engineering and Technology (CUET), Chittagong-4349, Bangladesh
[2]Bangladesh University of Engineering and Technology (BUET), Dhaka-1000, Bangladesh
E-mail: [1]ali.mehidi93@gmail.com, [2]maalim@math.buet.ac, [2]raity11@gmail.com*

Abstract

The boundary layer of momentum, energy and concentration has been analyzed for the effect of various dimensionless parameters such as magnetic parameter, pressure gradient parameter, stretching parameter and permeability parameter. In this regard, the governing partial differential equations are transformed into ordinary differential equations by applying local similarity transformations. The numerical results has been presented graphically which illustrate that the momentum boundary layer thickness reduces for increasing values of stretching ratio parameter, pressure gradient parameter and magnetic parameter but the thickness increases for curvature parameter and the heat transfer rate increases for increasing values of Prandtl number, Brownian motion parameter and stretching ratio parameter as a result the thermal boundary layer thickness decreases but reverse trend arises for thermophoresis parameter. Again the concentration decreases for increasing values of thermophoresis parameter but increases for Brownian motion parameter, pressure gradient and radius of curvature parameter. Therefore, the pressure gradient parameter, thermophoresis parameter and stretching ratio parameter is the key factor to enhance momentum, heat and mass transfer rate.

Keywords: MHD, Pressure gradient, Stretching ratio, Permeability.

1. Introduction

The boundary layer theory is important for many engineering field and real world problem. The main application of this theory is to find the skin friction drag acting on a body moving through a fluid, such as the drag of an airplane wing, a turbine blade, or a complete ship. So on the basis of Prandtl boundary layer theory, Falkner – Skan developed a model which is known as wedge flow. Therefore a lot of work has been done over the last few years. Among them are, Nield and Kuznetsov [1] and Kuznetsov and Nield [2] investigated the natural convective boundary layer flow of a nanofluid employing Buongiorno model. By applying the model of Nield and Kuznetsov [1], Khan and Pop [3] was first studied the boundary layer flow of nanofluid past a linearly stretching sheet. Mutuku [4] has discussed MHD boundary layer flow over a permeable vertical plate with convective heating' The boundary layer flow and heat transfer over a linearly stretching sheet with convective boundary condition in a nanofluid has been described by Makinde and Aziz [5]. Rana and Bhargava [6] has shown the steady, laminar boundary layer flow due to the nonlinear stretching flat surface in a nanofluid. Kandasamy et al. [7] investigated the MHD boundary layer flow of a nanofluid past a vertical stretching permeable surface with suction/injection. Mustafa et al. [8] analyzed the effect of various parameters in a nanofluid near a stagnation point towards a stretching surface. Later, Makinde et al. [9] discussed the combined effects of buoyancy force and magnetic field on stagnation-point flow and heat transfer in a nanofluid flow towards a stretching sheet. In view of the importance, the present work has focused on steady MHD forced convection, heat and mass transfer flow of an incompressible electrically conducting fluid over a stretching wedge in cylindrical coordinate.

2. Governing Equations and Similarity Analysis

Let us consider steady two dimensional MHD free convection heat and mass transfer in an incompressible electrically conducting fluid flow over a stretching wedge surface under the influence of an applied uniform magnetic field. The flow is subjected to a transverse magnetic field of strength B_0 which is assumed to be applied in the positive *y* –direction normal to the surface. Let us consider the steady axisymmetric flow of an incompressible fluid along a stretching wedge in presence of uniform magnetic field. Stretching velocity is produced by applying two equal and opposite forces on the surface such that the origin is kept at constant. The

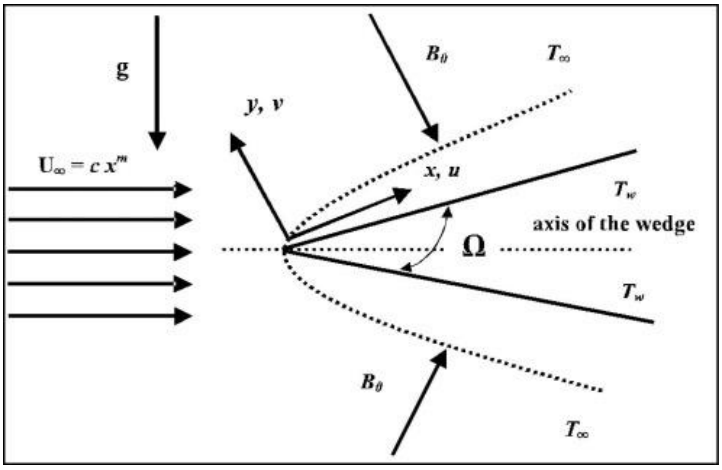

Fig. A. Flow configuration along the stretching wedge and the coordinate system

temperature of the surface $T_w(x)$ is higher than the ambient fluid temperature T_∞. The cylindrical coordinates are chosen in such a way that z-axes is taken along the axial direction of wedge surface while r-axis is perpendicular to it. Therefore, the z -axis is measured along the wedge surface and r -axis is measured in the radial direction which are shown in Fig.A. Let u_z and u_r be the velocity components along the surface and its radial direction. It is assumed that the free stream and the stretching velocity are $U = bz^m$ and $u_z = az^m$ respectively. Where a and b are the constant and m is the pressure gradient.

Equation of continuity:

$$\frac{\partial u_z}{\partial z} + \frac{u_r}{r} + \frac{\partial u_r}{\partial r} = 0 \tag{1}$$

Momentum equation:

$$u_z \frac{\partial u_z}{\partial z} + u_r \frac{\partial u_z}{\partial r} = U \frac{dU}{dz} + \nu_f \left(\frac{\partial^2 u_z}{\partial r^2} + \frac{1}{r}\frac{\partial u_z}{\partial r} \right) + \frac{\sigma B_0^2 \left(U - u_z\right)}{\rho_f} \tag{2}$$

Energy Equation:

$$u_z \frac{\partial T}{\partial z} + u_r \frac{\partial T}{\partial r} = \alpha_f \left(\frac{\partial^2 T}{\partial r^2} + \frac{1}{r}\frac{\partial T}{\partial r} \right) + \tau \left\{ D_B \left(\frac{\partial T}{\partial r}\frac{\partial C}{\partial r} \right) + \frac{D_T}{T_\infty} \left(\frac{\partial T}{\partial r} \right)^2 \right\} \tag{3}$$

Concentration Equation: [1]

$$u_z \frac{\partial C}{\partial z} + u_r \frac{\partial C}{\partial r} = D_B \left(\frac{\partial^2 C}{\partial r^2} + \frac{1}{r}\frac{\partial C}{\partial r} \right) + \frac{D_T}{T_\infty} \left(\frac{\partial^2 T}{\partial r^2} + \frac{1}{r}\frac{\partial T}{\partial r} \right) \tag{4}$$

Boundary conditions are:

$$u = u_z = az^m, T = T_w, C = C_w \text{ at } r = R$$

$$u = u_e = U = bz^m, T \to T_w, C \to C_w \text{ as } r \to \infty$$

To convert the governing equations into a set of similarity equations, we introduce the following similarity transformation with the steam function $\psi(x,y)$ such that

$$\eta = \left(\frac{r^2 - R^2}{2R}\right)\sqrt{\frac{U(1+m)}{2z\nu}},\ \psi = \sqrt{\frac{2z\nu U}{(1+m)}}Rf(\eta), \theta(\eta) = \frac{T - T_\infty}{T_w - T_\infty}, \varphi(\eta) = \frac{C - C_\infty}{C_w - C_\infty},$$

$$u_z = \frac{1}{r}\frac{\partial \psi}{\partial r} \quad and \ u_r = -\frac{1}{r}\frac{\partial \psi}{\partial z}$$

From the above transformations, the non-dimensional, nonlinear and coupled ordinary differential equations are obtained as follows:

$$(1+2\gamma\eta) f''' + \left(\frac{1+m}{2}\right) ff'' + \sqrt{2(1+m)}\gamma f'' + m(1 - f'^2) + \lambda M(1 - f') = 0 \tag{5}$$

$$(1+2\gamma\eta)\theta'' + \Pr(1+2\gamma\eta) Nt\ \theta'^2 + \frac{Nb}{Le}(1+2\gamma\eta)\theta'\varphi' + \frac{1}{2}\Pr(1+m) f\theta' + \sqrt{2(1+m)}\gamma\theta' = 0 \tag{6}$$

$$(1+2\gamma\eta)\varphi'' + (1+2\gamma\eta)\frac{Nt}{Nb}\theta'' + \frac{\sqrt{2(1+m)}\gamma Nt}{Nb}\theta' + \sqrt{2(1+m)}\gamma\varphi' + \frac{1}{2}Sc(1+m) f\varphi' = 0 \tag{7}$$

The transform boundary conditions:

$$f = 0,\ f' = \lambda, \theta = \varphi = 1 \ at \ \eta = 0$$

$$f' \to 1, \theta \to 0, \varphi \to 0 \ as \ \eta \to \infty$$

Where $f', \theta \ and \ \varphi$ are the dimensionless velocity, temperature and concentration respectively, η is the similarity variable, η_∞ is the value of η at which boundary conditions is achieved, the prime denotes differentiation with respect to η.

$$\gamma = \frac{1}{R}\sqrt{\frac{2\nu z}{U(1+m)}}, Nt = \frac{\tau D_T (T_w - T_\infty)}{\nu T_\infty}, Nb = \frac{\tau D_B (C_w - C_\infty)}{\nu}, \Pr = \frac{\nu}{\alpha},$$

$$Sc = \frac{\nu}{D_B}, Le = \frac{\alpha}{D_B}, m = \frac{\beta}{2-\beta}, \lambda = \frac{a}{b}, M = \frac{\sigma B_0^2 z}{\rho U}.$$

These are the radius of curvature, thermophoresis parameter, Brownian motion parameter, Prandtl number, Schmidt number, Lewis number, pressure gradient, velocity ratio and magnetic parameter respectively.

3. Results and Discussion

The velocity profiles for various dimensionless parameters have been shown in Fig. 1 – Fig.3. From these figures it is observed that the fluid velocity increases for increasing values of magnetic parameter, pressure gradient parameter and curvature parameter which produces larger skin friction coefficient as a result the boundary layer thickness reduces but the reverse result arises in case of stretching ratio parameter.

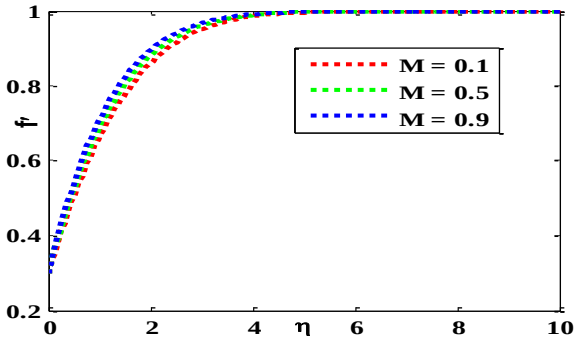

Fig.1. Velocity profiles for various values of M

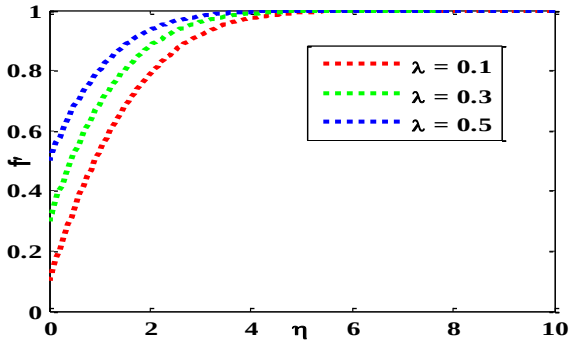

Fig.2.Velocity profiles for various values of λ

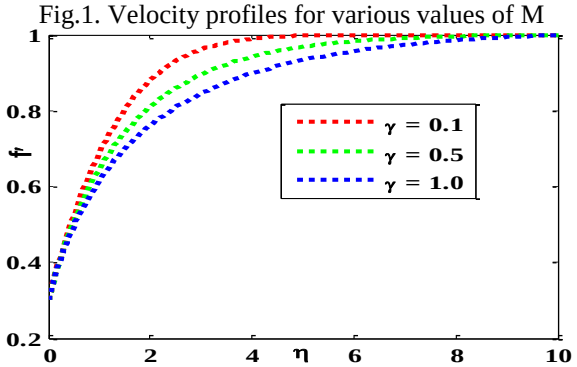

Fig.3. Velocity profiles for various values of γ

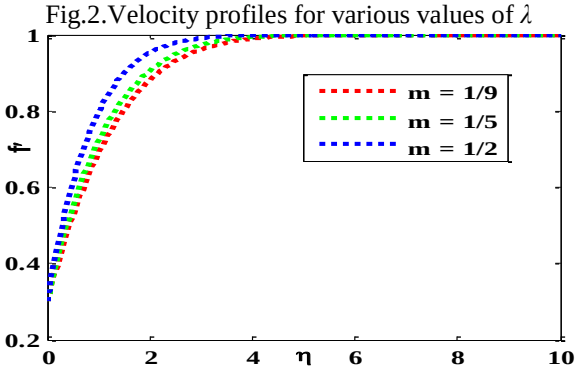

Fig.4. Velocity profiles for various values of m

The temperature profiles for various dimensionless parameters have been shown in Fig. 5 – Fig.8. From these figures it is observed that the temperature within the boundary layer increases for increasing values of Brownian motion and curvature parameter as a result the thermal boundary layer thickness increases because the heat transfer rate decreases but the reverse results arises in case of stretching ratio parameter, and thermophoresis parameter because the heat transfer rate increases.

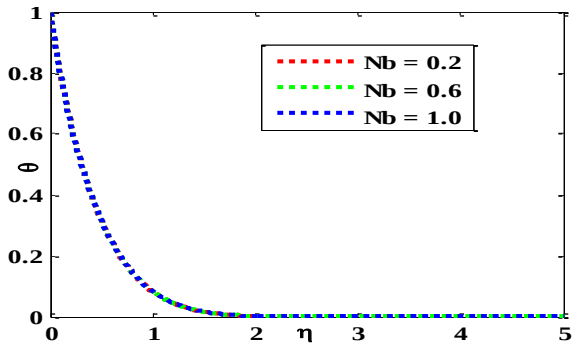

Fig.5. Temperature profiles for various values of Nb

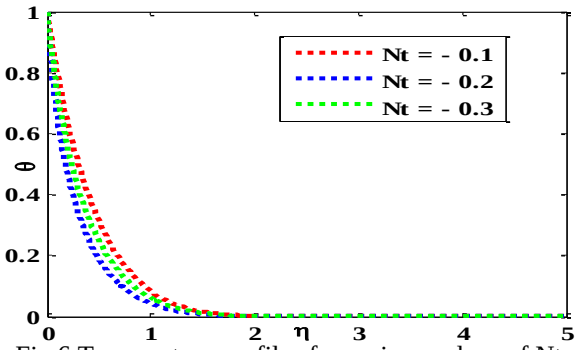

Fig.6.Temperature profiles for various values of Nt

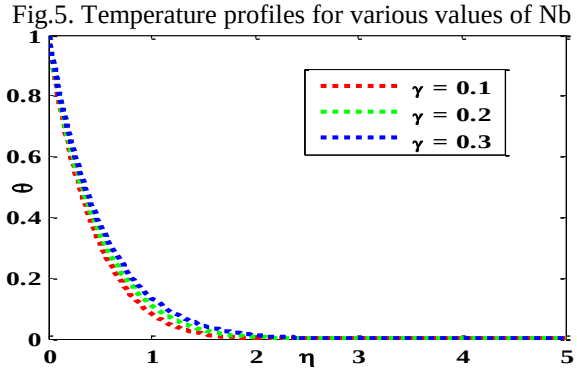

Fig.7. Temperature profiles for various values of γ

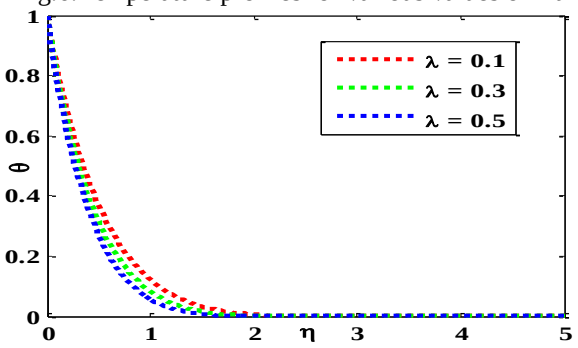

Fig.8. Temperature profiles for various values of λ

Again, the concentration profiles for various dimensionless parameters have been depicted in Fig. 9 – 12. From these figures it is observed that the concentration within the boundary layer increases for increasing values of pressure gradient parameter, curvature parameter and Brownian motion parameter, as a result the concentration

boundary layer thickness increases because the mass transfer rate decreases but the reverse results arises in case of thermophoresis parameter because the mass transfer rate increases.

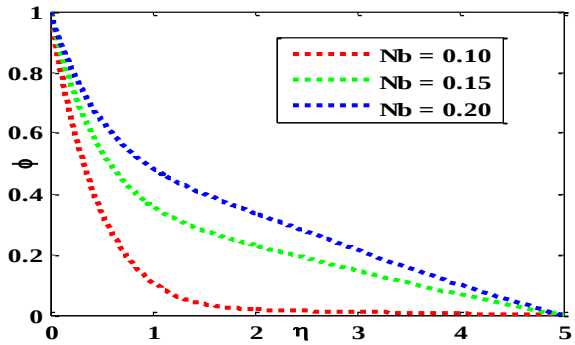

Fig.9. Concentration profiles for various values of Nb

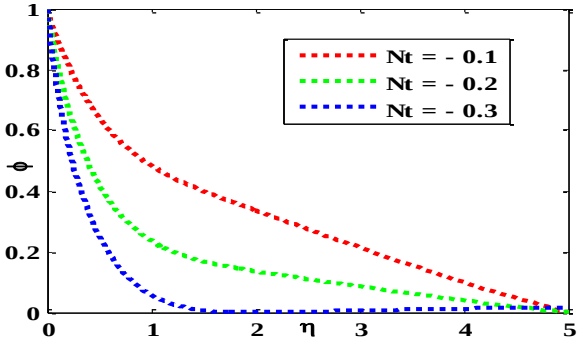

Fig.10.Concentration profiles for various values of Nt

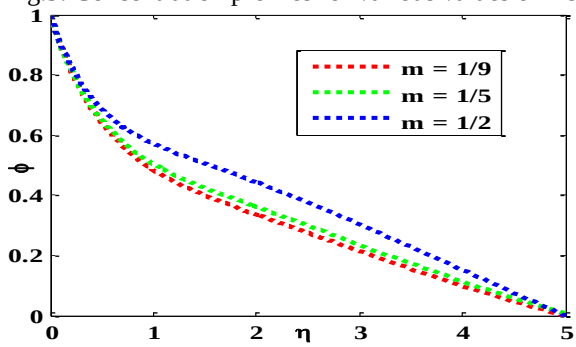

Fig.11. Concentration profiles for various values of m

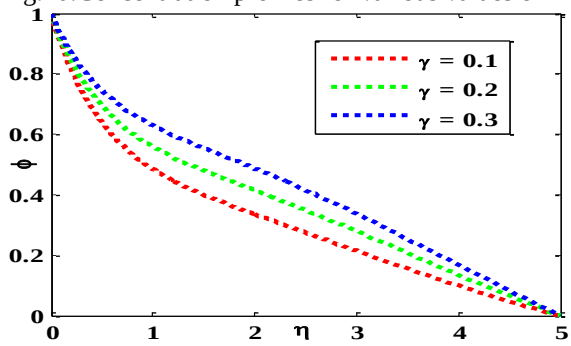

Fig.12. Concentration profiles for various values of γ

4. Conclusions

Following are the conclusions made from above analysis:

- The momentum boundary layer thickness reduces for increasing values of magnetic parameter, pressure gradient parameter and curvature parameter. Again, the thickness increases for the increasing values of stretching ratio parameter.

- The thermal boundary layer thickness increases for Brownian motion and curvature parameter because the heat transfer rate decreases but the reverse results arises in case of stretching ratio parameter, and thermophoresis parameter because the heat transfer rate increases.
- Again, for increasing values of pressure gradient parameter, curvature parameter and Brownian motion, the concentration boundary layer thickness increases because the mass transfer rate decreases but the reverse results arises in case of thermophoresis parameter because the mass transfer rate increases.

5. References

[1] D. A. Nield and A. V. Kuznetsov, "The Cheng-Minkowycz problem for natural convective boundary-layer flow in a porous medium saturated by a nanofluid", *International Journal of Heat Mass Transfer*, Vol. 52, pp. 5792–5795, (2009).

[2] A. V. Kuznetsov and D. A. Nield, "Natural convective boundary layer flow of a nanofluid past a vertical plate", *International Journal of Thermal Science*, Vol. 49, pp. 243–247, (2010).

[3] W. A. Khan and I. Pop, "Boundary-layer flow of a nanofluid past a stretching sheet", *International Journal of Heat Mass Transfer*, Vol. 53, pp. 2477–2483, (2010).

[4] W. N. Mutuku-Njane and O. D. Makinde, "MHD nanofluid flow over a permeable vertical plate with convective heating", *Journal of Computational and Theoretical Nano science*, Vol. 11, pp. 667–675, (2014).

[5] O. D. Makinde and A. Aziz, "Buoyancy effects on MHD stagnation point flow and heat transfer of a nanofluid past a convectively heated stretching/shrinking sheet", *International Journal of Thermal Sciences*, Vol. 50, No. 7, pp. 1326-1332, 2011.

[6] P. Rana and R. Bhargava, "Numerical simulation of nanofluids based on power-law fluids with flow and

heat transfer", *Communication Nonlinear Science and Numerical Simulation*, Vol. 17, No.1, pp. 212-226, 2011.

Nomenclature

MHD	megnetohydrodynamic
α_f	thermal diffusivity of the base fluid, mm^2s^{-1}
κ	thermal conductivity, w $m^{-1}K^{-1}$
g	acceleration due to gravity, ms^{-2}
σ	electrical conductivity, sm^{-1}
D_B	Brownian diffusion coefficient
D_T	thermophoresis diffusion coefficient
ν_f	kinematics viscosity of the base fluid, m^2s^{-1}
ρ_f	density of base fluid, kg m^{-3}
B_0	magnetic field intensity, Am^{-1}
u	velocity component along x axis, ms^{-1}
a	stream velocity constant
v	velocity component along y axis, ms^{-1}
b	free stream velocity constant
m	pressure gradient
τ	ratio of the effective heat capacity
λ	stretching ratio
γ	radius of curvature
C	nanoparticle volume fraction, kg m^{-3}
C_w	plate volume fraction, kg m^{-3}
C_∞	free stream nanoparticle volume fraction
T	fluid temperature, k^{-1}
T_w	plate temperature, k^{-1}
T_∞	free stream temperature
ψ	stream function